Coupled channel vector-boson scattering in the N/D method

Duane A. Dicus
Center for Particle Physics and Department of Physics, University of Texas, Austin, Texas 78712

Vigdor L. Teplitz
Physics Department, Southern Methodist University, Dallas, Texas 75275
(Received 14 April 1993; revised manuscript received 28 February 1994)

We consider the two coupled channels $V_L V_L$ and HH where H is the Higgs boson and V_L the longitudinal vector boson. We unitarize the tree diagram amplitudes using the coupled channel N/D method and compute s- and p-wave scattering amplitudes for a range of Higgs boson mass values. We also find values for the Higgs boson mass at which the potential is sufficiently strong to give a bound state below the VV threshold (around 1.2 TeV for one choice of potential term).

PACS number(s): 11.50.Ec, 11.15.Ex, 14.80.Er, 14.80.Gt

I. INTRODUCTION

Knowledge of deviations of vector-boson scattering from lowest-order electroweak perturbation theory predictions is essential for accurate interpretation of future proton-proton collider results for vector-boson production. Toward this end a number of authors have computed corrections for various values of the Higgs boson mass using various approaches. Such efforts include the original calculation of Dicus and Mathur [1] showing that, for sufficiently large Higgs boson mass unitarity would be violated, the influential calculation by Lee, Quigg, and Thacker [2] of longitudinal vector-boson scattering and related processes in the N/D "determinantal" approximation, the N/D calculation of Contogouris *et al.* [3] of the Higgs boson as a "bootstrapped" bound state of HH scattering and as a resonance in ZZ scattering, the N/D calculation of Hikasa and Igi [4] of H as an N/D "bootstrapped" bound state in vector-boson scattering, the N/D calculation of Sivers and Uretsky [5] of the same nature but with different assumptions including, importantly a free parameter in a subtraction constant, the s-wave K-matrix unitarization by Repko and co-workers [6], analytic approximations to unitarity using Padé approximants by Truong *et al.* [7], s-wave and p-wave unitarization by Dicus and Repko [8] using Padé approximants, s- and p-wave unitarization by Veltman and Veltman [9] by carrying over pion-pion scattering results, a Hamiltonian model for the Higgs resonance by Chiu, Sudarshan, and Bhamathi [10], self-consistent calculations using a Padé approximant unitarization scheme by Balázs [11], a comparison of pion-pion and vector-boson scattering results by Atkinson, Harada, and Sanda [12], and a study of the effects of final-state interactions by Basdevant *et al.* [13].

Our calculations in this paper use the N/D method. The defining property of the method is that, given a potential, it produces an amplitude that satisfies a unitarity condition and has the same discontinuity across the left-hand cut as that of the potential. Our unitarity condition is that of elastic unitarity in the two coupled channels $V_L V_L$ and HH where V_L is a longitudinal vector boson. The HH channel is an important one because the potential rises as m_H^4, although the effect is damped by the $4m_H^2$ increase of the elastic threshold. As Lee, Quigg, and Thacker [2] point out, however, the H lifetime decreases rapidly (m_H^{-5}) with increasing m_H, casting doubt on the validity and interpretation of HH scattering results.

We adopt the viewpoint that while the H lifetime falls with m_H, HH scattering increases and at the same time $V_L V_L$ scattering into inelastic channels rises with the HH intermediate state potentially a major contributor. We thus consider the inclusion of the HH intermediate state potentially an improvement over the consideration of only $V_L V_L$ elastic scattering. To some extent, effects of inelasticity are independent of the details of the inelasticity. Specifically the opening of inelastic channels provides increased attraction in the lowest threshold channel so that, at the very least, inclusion of the HH intermediate state should provide qualitative insight.

A second thorny issue is that of (unknown) subtraction constants in the s-wave dispersion relation. Within the standard model (SM), s-wave $V_L V_L$ scattering is calculable in low order with no undetermined parameters; however, for a large Higgs boson mass it must be unitarized by higher-order diagrams. These corrections do not "hold fixed" $V_L V_L$ scattering at any point. Thus, if we made a subtraction at the symmetry point

$$s = t = u = \tfrac{4}{3} m_V^2 , \tag{1.1}$$

where for $p_1 + p_2 \to p_3 + p_4$ we make the conventional definitions

$$\begin{aligned} s &= (p_1 + p_2)^2 , \\ t &= (p_1 - p_3)^2 , \\ u &= (p_1 - p_4)^2 , \end{aligned} \tag{1.2}$$

it would not be correct to set the amplitude for $V_L V_L$

scattering at the symmetry point equal to its tree-diagram approximation.

At least two approaches to the subtraction constant problem are possible. (1) We can (and will) assume no subtraction is needed. We will calculate within the N/D "strip approximation" [14] in which numerical results are achieved without a numerical need for a subtraction to eliminate divergences; within that approximation numerical results are relatively insensitive to the width of the strip. (2) Alternatively, we could make a subtraction and then attempt to relate the subtraction parameter to a physical quantity as, for example, Sivers and Uretsky do in adjusting m_H and the subtraction constant so as to reproduce the Higgs position and width. We adopt the first approach with the aim of providing readily comparable numerical experiments by varying the input potential.

We are thus led to a third related issue, the form of the potential to be unitarized. Three choices present themselves immediately; others are possible.

(a) We can compute V^J_{HH}, V^J_{VH}, and V^J_{VV} for the coupled reactions $HH\to HH$, $V_LV_L\to HH$, and $V_LV_L\to V_LV_L$ for high J and analytically continue to low J. This procedure intentionally omits contact and direct channel pole terms. Its virtue is that it takes from the SM only the quantum numbers of the particles of interest and the relation between the couplings of the exchange particles and m_H.

(b) We can add, to the potential matrix above, the s-channel elementary particle corresponding to the Higgs boson. We do this by adding a pole to V with the Higgs position and residue.

(c) We can add, to the potential matrix above, the constant contribution necessary to reproduce the full tree amplitudes.

Below we solve the coupled channel N/D equations for all three choices. Our goal is to aid in providing assistance to those involved in preparing to search for a heavy Higgs boson at the CERN Large Hadron Collider (LHC). Toward this end we consider three questions.

(1) Onset of low-mass s-wave bound states. For m_H sufficiently large the attractive force should give rise to a s-wave bound state in V_LV_L scattering. Such a bound state would appear to be an intermediate mass (or low mass) Higgs boson. However, a theory with an elementary H with a mass m_H so large as to predict the presence of an absent particle would not make sense. If a value of m_H above which a V_LV_L bound state is predicted could be established, we could limit the Higgs boson search to masses below that value. It then makes sense to attempt to compute such a mass value with a variety of different unitarization methods (in the absence of a single compelling one).

(2) Unitarized V_LV_L scattering amplitudes. As m_H increases, the residue of its pole increases and it becomes increasingly difficult to establish from VV production the existence of an s-wave pole. Again it appears to us useful to compute V_LV_L scattering with a variety of unitarization methods, including the N/D method.

(3) p-wave and $I=2$ scattering. A partial-wave analysis of W_LW_L production will not be easy. It therefore appears useful to compute p-wave scattering as well as s-wave scattering in order to determine plausible ranges for corrections to the s-wave predictions. We note that s-wave exchanges do not produce p-wave resonances and we do not consider in this paper bootstrapping p-wave resonances. Finally we address as well isospin two scattering which is needed for predicting $W^\pm_LW^\mp_L$, Z_LZ_L, and $W^\pm_LW^\pm_L$.

Our objective is to study the questions cited using the three potentials discussed above. Section II gives the details of the formalism. Section III describes the numerical computations and their results. Section IV has a discussion of these results.

II. FORMALISM

We proceed in the approximation of degenerate Z and W, $m_W=m_Z=m_V$. We do not set m_W/m_H to zero. We consider the amplitudes $A^{I=0}_{J=0}(V_LV_L\to V_LV_L)$, $A_{J=0}(V_LV_L\to HH)$, $A_{J=0}(HH\to HH)$, $A^{I=2}_{J=0}(V_LV_L\to V_LV_L)$, and $A^{I=1}_{J=1}(V_LV_L\to V_LV_L)$.

We write each amplitude A as N/D, where D's singularities are those required by unitarity (for positive energies) at thresholds while N has all the singularities but those of D. With this decomposition it is well known [14] that an integral equation for N can be written and that D can be found from N. The density of states factor ρ, for the s-wave V_LV_L, s-wave HH, and p-wave V_LV_L, systems are

$$\rho_{0V}(s)=\tfrac{1}{2}(1-4m_V^2/s)^{1/2}\,, \tag{2.1}$$

$$\rho_{0H}(s)=\tfrac{1}{2}(1-4m_H^2/s)^{1/2}\,, \tag{2.2}$$

$$\rho_{1V}(s)=(s-4m_V^2)^{3/2}/(8s^{1/2})\,. \tag{2.3}$$

We note that our phase space factors correspond to a choice of elastic scattering of the form $(W/q)e^{i\delta}\sin\delta$ while the Lee, Quigg, and Thacker [2] choice is $(W/2q)e^{i\delta}\sin\delta$. Thus our potentials in (2.6)–(2.10) below, where comparable, are twice those of Lee, Quigg, and Thacker. The N/D equations are

$$N(s)=V(s)+\frac{1}{\pi}\int_{\rm RHC}ds'\frac{V(s')-V(s)}{s'-s}\rho(s')N(s')\,, \tag{2.4}$$

$$D(s)=1-\frac{1}{\pi}\int_{\rm RHC}ds'\frac{\rho(s')N(s')}{s'-s}\,, \tag{2.5}$$

where V is the input "potential" with no right-hand cut (RHC). The N/D method is such that, along the left-hand cut, $\operatorname{disc}A\equiv\operatorname{disc}(ND^{-1})=\operatorname{disc}V$, as can be seen from Eqs. (2.4) and (2.5) while along the RHC $\operatorname{disc}A=\rho|A|^2=\operatorname{Im}A$.

We take the potentials for the five amplitudes from standard model tree diagrams; thus we have, letting $\lambda_M=2G_Fm_H^2/(8\pi\sqrt{2})$,

$$V^{I=0}_{J=0}(s)=\lambda_M\left[\frac{m_H^2}{4v_V}\ln(1+4v_V/m_H^2)-\frac{3}{2}\frac{m_H^2}{s-m_H^2}\alpha_P-\frac{5}{2}\alpha_4\right]\,, \tag{2.6}$$

$$V^{V,H}_{J=0}(s)=\left[\frac{3}{2}\right]^{1/2}\lambda_M\left[\frac{F}{2p_Hq_V}\ln\left[\frac{z_1+1}{z_1-1}\right]+3\frac{m_H^2}{s-m_H^2}\alpha_P+\alpha_4\right], \tag{2.7}$$

$$V^{H}_{J=0}(s)=3\lambda_M\left[\frac{3m_H^2}{2\nu_H}\ln(1+4\nu_H/m_H^2),-3\frac{m_H^2}{s-m_H^2}\alpha_P-\alpha_4\right], \tag{2.8}$$

$$V^{I=1}_{J=1}(s)=\lambda_M\frac{m_H^2}{2\nu_V}Q_1(1+4\nu_V/m_H^2), \tag{2.9}$$

$$V^{I=2}_{J=0}(s)=\lambda_M\left[\frac{m_H^2}{4\nu_V}\ln(1+4\nu_V/2m_H^2)-\alpha_4\right], \tag{2.10}$$

where $q_V^2=\nu_V=(s-4m_V^2)/4$, $p_H^2=\nu_H=(s-4m_H^2)/4$, $s=(p_1+p_2)^2=4(p_H^2+m_H^2)=4(q_V^2+m_V^2)$, Q is a Legendre function of the second kind, and

$$F=1-4m_V^2/m_H^2+2sm_V^2/m_H^4 \tag{2.11}$$

and the three cases ($\alpha_P=\alpha_4=0$), ($\alpha_P=1,\alpha_4=0$), and ($\alpha_P=\alpha_4=1$) correspond to taking the $J=0$ potential to be the result of analytic continuation only, analytic continuation plus the addition of a (direct-channel) elementary particle, and the full field theory tree amplitude, respectively. Additionally, we have

$$z_1=(m_H^2-s/2)/(2p_Hq_V). \tag{2.12}$$

The solution of (2.4) and (2.5), with potentials $V^{I=1}_{J=1}$ and $V^{I=2}_{J=0}$ (and phase space factors ρ_{1V} and ρ_{0V}) then yield the amplitudes $A^{I=1}_{J=1}$ and $A^{I=2}_{J=0}$. The $I=0$, $J=0$ amplitudes give rise to coupled equations as follows:

$$N_{ij}(s)=V_{ij}(s)+\frac{1}{\pi}\int_{\rm RHC}ds'\frac{V_{ik}(s')-V_{ik}(s)}{s'-s}\rho_k(s')N_{kj}(s'), \tag{2.13}$$

$$D_{ij}(s)=1-\frac{1}{\pi}\int_{\rm RHC}\frac{ds'}{s'-s}\rho_i(s')N_{ij}(s'), \tag{2.14}$$

$$A_{ij}(s)=N_{ik}(s)[D(s)]^{-1}_{kj}, \tag{2.15}$$

where (i,j) equals (1,2) for (HH,V_LV_L). It can be shown that V_{ij} being symmetric implies A_{ij} is symmetric.

Partial wave cross sections are given by

$$\sigma_J=\frac{4\pi(2J+1)}{k^2}(\rho A)^2, \tag{2.16}$$

where k is the c.m. momentum. Bound state poles correspond to zeros of D. Their coupling constants (and widths) are given by

$$\Gamma_s=N(s_0)\Big/\left[\frac{\partial D}{\partial s}\bigg|_{s=s_0}\right]=2W\Gamma_W, \tag{2.17}$$

where $W=\sqrt{s}$ is the total c.m. energy [15].

For completeness we note that amplitudes for $W_L^+W_L^-$ scattering and Z_LZ_L scattering are given by

$$(W_L^+W_L^-\to W_L^+W_L^-)=\tfrac{1}{3}A^{I=0}+\tfrac{1}{2}A^{I=1}+\tfrac{1}{6}A^{I=2}, \tag{2.18}$$

$$(W_L^+W_L^-\to Z_LZ_L)=-\tfrac{1}{3}A^{I=0}+\tfrac{1}{3}A^{I=2}, \tag{2.19}$$

$$(Z_LZ_L\to Z_LZ_L)=\tfrac{1}{3}A^{I=0}+\tfrac{2}{3}A^{I=2} \tag{2.20}$$

and that, in deriving the potentials above and in the discussion below, we have used the crossing matrix of Chew and Mandelstam [16]:

$$\alpha_{II'}=\begin{bmatrix}2/3 & 2 & 10/3\\ 2/3 & 1 & -5/3\\ 2/3 & -1 & 1/3\end{bmatrix}. \tag{2.21}$$

Consider the meaning of the factors α_P and α_4 in (2.6)–(2.10). If α_P and α_4 are both 1, these equations simply reproduce the tree-diagram approximation to the (one Higgs doublet) standard model amplitudes. Solution of the N/D equations then constitutes one method for adding higher-order contributions, specifically those parts of loop diagrams with two-body threshold singularities. If both α_P and α_4 are zero, (2.6)–(2.10) give the results of analytic continuation of the potential, in complex J, from high J (for which there are no direct channel bound states or resonance contribution, no one vertex diagram contribution, and no terms nonanalytic in J induced by cross channel pole spin factors) to low J. The result of this continuation is to subtract from the $\alpha_P=\alpha_4=1$ potentials those contributions just cited—the direct channel Higgs pole, the various one vertex four point Higgs diagrams, and an extra constant term that arises from the coupling of the exchanged Higgs scalar to spin one particles. That is, write $t/(t-m_H^2)=1+m_H^2/(t-m_H^2)$; with $\alpha_4=0$ only the second term on the right-hand side (RHS) is kept. Use of this potential constitutes an attempt to "bootstrap" the physical Higgs boson.

If there is a value of m_H for which the result of solving the N/D equations (for the $\alpha_P=\alpha_4=0$ potential) is to give an s-wave bound state at m_H, with the same coupling to H and V assumed in computing the crossed Higgs pole contribution to HH and VV scattering, that value would be a unique self-consistent one. For that value of m_H the scattering amplitudes would be analytic in the J plane and the Higgs boson would lie on a Regge trajectory. If this were to happen, the scattering amplitude would be completely determined by specifying the particle content of the theory and enforcing the requirements of unitarity and analyticity, but there would be no assurance that the corresponding field theory is renormalizable. Choosing $\alpha_P=1$, and $\alpha_4=1$ specifies a theory in which the scattering amplitude is analytic in J except for the contribution of an elementary s-channel Higgs boson [related to a Castillejo-Dalitz-Dyson (CDD) pole [17]]. Lee, Quigg, and Thacker [2] consider only the $\alpha_P=\alpha_4=1$ possibility, while Contogouris *et al.* [3] search for a bootstrap solution with only the $\alpha_P=\alpha_4=0$ possibility. We provide results for all three cases.

III. CALCULATIONS

Our calculations were performed on a Vax 6420 using the routine LINRG from the IMSL.MATH library to invert the matrix approximation to the one-channel and two-channel integral equations (2.4) and (2.13). For the single channel case we approximated the kernel of (2.4) by a 100×100 matrix; for the coupled channel case we used 100 s-values in each channel for a total of 200×200.

A. $I=0$ scattering

We begin with coupled channel, $I=0$ scattering for which we looked at four possibilities for the two by two (V_LV_L, HH) potential matrix (2.6)–(2.8).

(A) $\alpha_P=\alpha_4=0$; no $V_LV_L\to HH$ coupling. Recalculating this case permitted checking against the single channel work of others, as well as providing a base line against which one can see the effects of more elaborate potentials.

(B) $\alpha_P=\alpha_4=0$ with V_LV_L-HH coupling as given in (2.7). This case corresponds to the classic "S-matrix theory" approach as described above.

(C) $\alpha_4=0$, and $\alpha_P=1$ (with V_LV_L-HH coupling). Here an elementary Higgs boson is explicitly introduced into the s channel.

(D) $\alpha_4=\alpha_P=1$ (with V_LV_L-HH coupling). This case corresponds to the full field theory potential of Lee, Quigg, and Thacker [2]. We augment it with the off-diagonal contributions as well.

These cases give rise to strikingly different potentials. For $V_LV_L\to V_LV_L$, for example, in cases (A) and (B), V is positive definite and approaches a nonzero constant at $s=4M_V^2$; in case (C), V has a pole at $s=m_H^2$, is negative just above the pole, and then returns to slowly decreasing positive values; in case (D), V is essentially linearly rising near $s=4M_V^2$ but above the pole at $s=m_H^2$ approaches a negative constant. Table I illustrates the wide variation.

The result of solving Eq. (2.13) for N, evaluating D from (2.14) and finding the zeros of D (poles of the scattering amplitude) is, for case (A) as follows. For small m_H, D has no zeros and is close to unity; correspondingly the full amplitude is close to that of the potential V. As m_H is increased from zero, a minimum in

$$D_i=1-\int_{s_i}^{\infty}ds'\frac{\rho_iN_i(s')}{s'-s}\quad(i=V_LV_L,HH)$$

develops near the threshold ($s_V=4m_V^2, s_H=4m_H^2$). For sufficiently large m_H (1.4 TeV) the minimum value of D goes negative so that the amplitude has a bound-state pole just below the threshold, the second, above threshold, zero of D represents a value of s for which the phase shift is falling through $\pi/2$, as required by Levinson's theorem [18], to its asymptotic value. No resonance is possible (with purely attractive potentials) for an s-wave channel since, with no centrifugal barrier, there can be no partially confining well. As m_H is further increased the bound-state pole moves to lower values for $s_B(m_H^2)/m_H^2$. s_B eventually goes negative.

In case (B), the result of the off-diagonal interaction is little change in the bound state near $4m_H^2$, but significant extra attraction in the effective V_LV_L channel so that the onset of the bound state comes at lower m_H (1.2 TeV vs 1.4 TeV). The result of case (B) is relatively little modified in passing to case (C). Case (D), however, is significantly different since the nonanalytic (in J) contact terms constitute a sizable repulsive potential. Positive V tends to give positive N and that makes D less than one; negative N values tend to make D greater than one precluding the zeros that represent bound states. Nevertheless, at low s, V is positive and rises linearly and for sufficiently large m_H bound-state poles appear (at $m_H=2.3$ TeV). These results are summarized in Table II.

We turn now to the $I=0, V_LV_L$ scattering amplitudes. In Figs. 1–4 we present the results for the $I=0$ amplitude, $(e^{2i\delta}-1)/2i$, discussed above.

(A) $\alpha_P=\alpha_4=0$, with $V(HH\to V_LV_L)$ set equal to zero, followed by three cases with $V(HH\to V_LV_L)$ not set to zero: (B) $\alpha_P=\alpha_4=0$; (C) $\alpha_P=1,\alpha_4=0$; (D) $\alpha_P=\alpha_4=1$. For each of these four cases we plot the potential and the real and imaginary parts of $(e^{2i\delta}-1)/2i$ for the range $W=2m_V$ to $W=2$ TeV. For completeness we note that, in our calculations, $2m_V=0.170$ TeV; our points begin at 0.175 and are calculated at intervals of 0.025 TeV. We truncate the curves for the potential at absolute value one.

Case (A): In Figure 1(a) $[m_H=0.5, V(HH\to V_LV_L)=0, \alpha_P=\alpha_4=0]$ we see an example of a general effect expected from unitarizing an attractive potential. Re A is slightly larger than V for low W and slightly less at high W. Figure 1(b) for $m_H=1.0$ TeV maintains the same general shape. In Figs. 1(c) and 1(d) we see the elastic VV amplitude falling through $\pi/2$ at 0.25 TeV and 0.6 TeV since, as discussed above, for $m_H>1.4$ TeV there is a bound-state pole, which is, of course, not shown because it lies below threshold. This, of course, raises the general point that if an intermediate mass "Higgs particle" is discovered below the $2m_V$ threshold, it will not be clear that such a particle corresponds to the Higgs boson in the standard model Lagrangian; conceivably there could be a high mass SM Higgs boson that produces

TABLE I. Selected values of the potential V for $V_LV_L\to V_LV_L$ for the four cases (A), (B), (C), and (D).

Higgs boson mass, s (in TeV)	(A),(B)	(C)	(D)
$m_H=1,\ s=0.2$	0.60	1.86	0.22
$m_H=1,\ s=6.0$	0.22	−0.02	−1.6
$m_H=2,\ s=0.2$	2.56	6.6	0.16
$m_H=2,\ s=6.0$	1.6	−7.4	−13.4

TABLE II. Approximate minimum values of the Higgs-boson mass m_H for which VV bound states appear.

Case	Minimum M_H (in TeV)
(A)	1.4
(B)	1.2
(C)	1.2
(D)	2.3

dynamically a VV bound state, as discussed further below.

Case (B): In Figs. 2(a) and 2(b) we see the effects of including the coupling to the HH channel, cusplike behavior for $\mathrm{Re}A$ in the lower mass channel at the higher threshold, 10 to 20% enhancement, step functionlike behavior for $\mathrm{Im}A$ at the threshold. In Fig. 2(b) we see a more radial enhancement over Fig. 1(b) because of proximity to the value (1.2 TeV) for m_H at which a bound-state pole develops in case (B).

Case (C): In Figs. 3(a)–3(d) we see that inclusion of the direct-channel, elementary particle pole does not greatly change the amplitude away from the pole: $\mathrm{Re}A$ and $\mathrm{Im}A$ Fig. 3(c), for example, agree with $\mathrm{Re}A$ and $\mathrm{Im}A$ in Fig. 2(c) to within about 0.01 for $|W-1.5|$ greater than 0.1 TeV. The similarity of the real and imaginary parts of the amplitudes in Figs. 2(d) and 3(d) (away from 2 TeV) is striking. In short, $V_L V_L$ scattering at energies *away* from a heavy Higgs pole is not indicative of the existence of an elementary Higgs boson.

Case (D): In Fig. (4) we see that the inclusion of the large, negative constant terms from the tree diagrams drives $\mathrm{Re}A$ negative and produces a significantly smaller amplitude. Because there is no bound state until $m_H=2.3$ TeV there is, of course, no sign of the large scattering amplitudes of Figs. 1(d), 2(c), 2(d), and 3(c). The change in sign of $\mathrm{Re}A$ between Figs. 3(c) and 3(d) is an indication of the approach to the value, $m_H=2.3$ TeV, at which there is a bound state.

In Figs. 5 and 6 we compare (for $\mathrm{Re}A$ and $\mathrm{Im}A$, respectively) the four different cases (A)–(D) cited above at the four different m_H. Again it stands out clearly that cases (B) and (C) (including off-diagonal potentials, without and with, respectively, the elementary particle pole, but without the constant terms) are very similar except at the pole itself. Case (A) is close to cases (B) and (C) except somewhat "less advanced" without the extra attraction from including coupling to the second channels. Figure 6(b) shows a dramatic rise for cases (B) and (C) in $\mathrm{Im}A$ near 2 TeV. This is a result of the fact that around $m_H=1$ TeV the HH channel develops a bound state just below threshold as shown in Ref. [3].

We checked the sensitivity of the above results on the amplitudes to the two "calculational parameters"—the upper limit of integration W_1^2 in Eqs. (2.4), (2.5), etc. (the "strip width") and the number of the 100 integration points N_1 chosen to lie between $2m_V$ and $2m_H$. We calculated the amplitudes for the 16 cases discussed above, for the nine combinations $W_1=(3,\ 6,\ \text{and}\ 9)m_H$ and

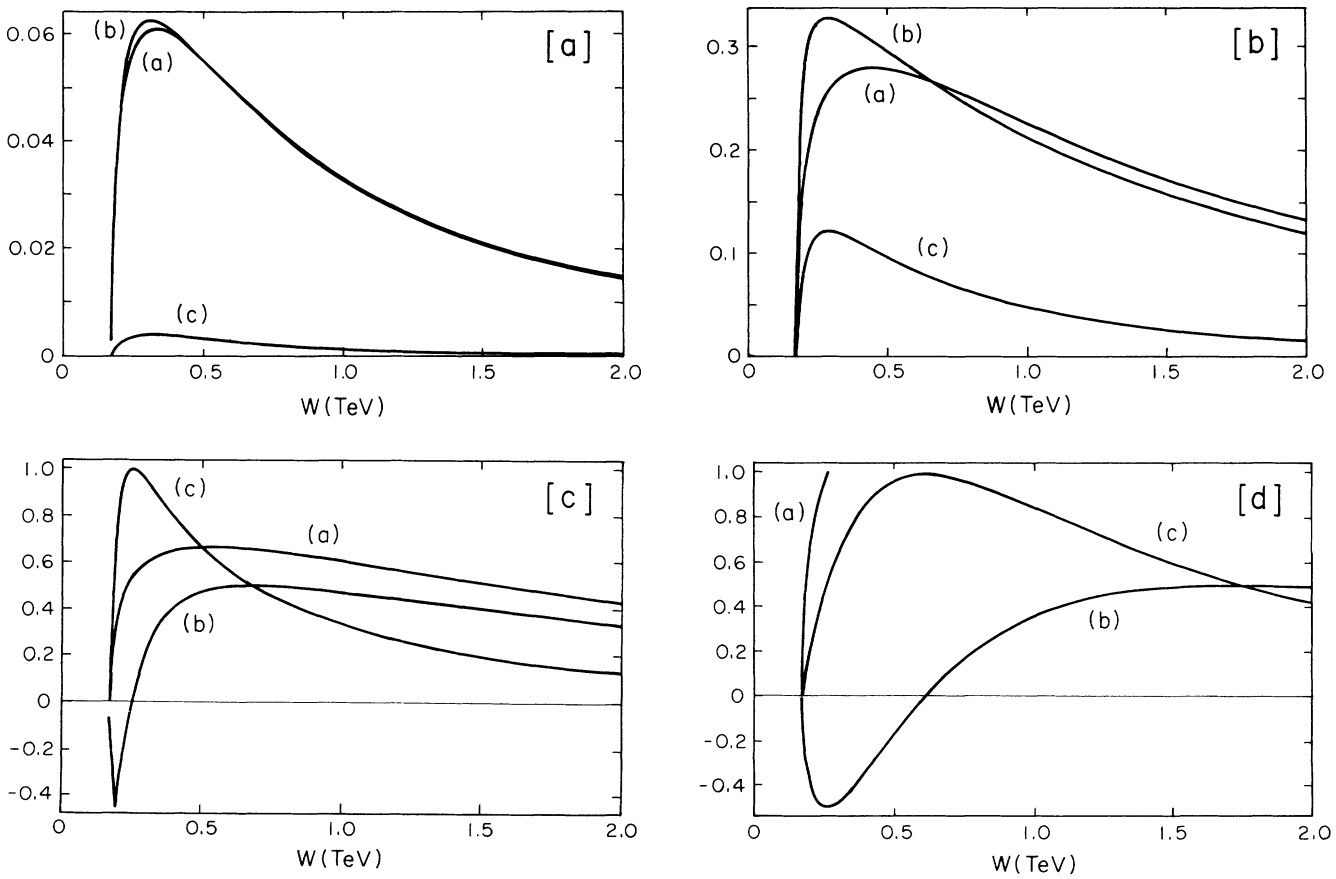

FIG. 1. The effect of unitarizing the $I=0$ amplitude with no $V_L V_L \to HH$ coupling. The curves (a), (b), (c) correspond to the potential, the real part of the amplitude, and the imaginary part of the amplitude. W is the c.m. energy. (a) assumes a Higgs boson mass of 0.5 TeV; (b), (c), and (d) assume m_H equal 1.0, 1.5, and 2.0 TeV.

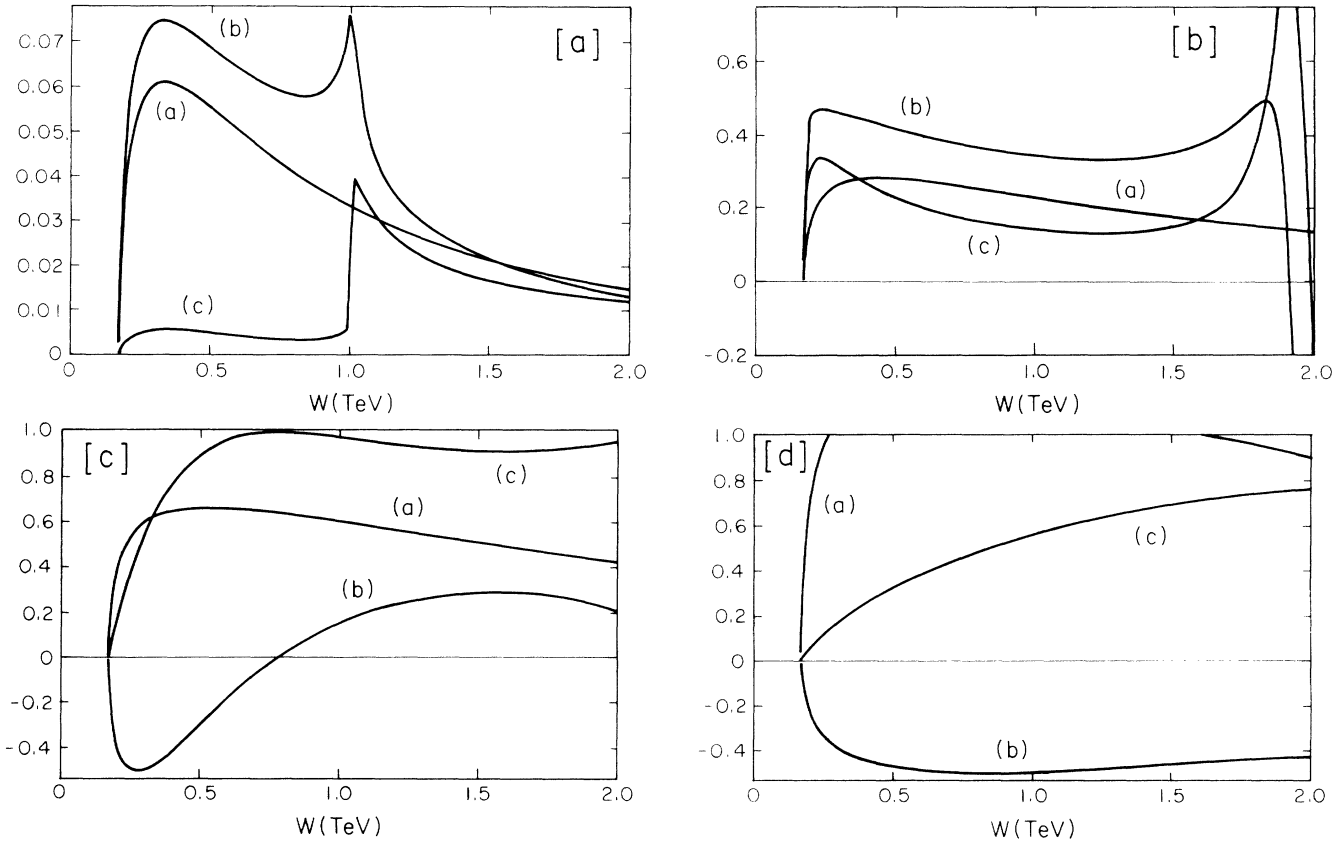

FIG. 2. The same as Fig. 1, but with $HH \to V_L V_L$ included. The potential is assumed to be the result of analytic continuation only, i.e., $\alpha_P = \alpha_4 = 0$ [see Eqs. (2.6)–(2.10)]. Again (a)–(d) assume m_H equal 0.5, 1.0, 1.5, and 2.0 TeV.

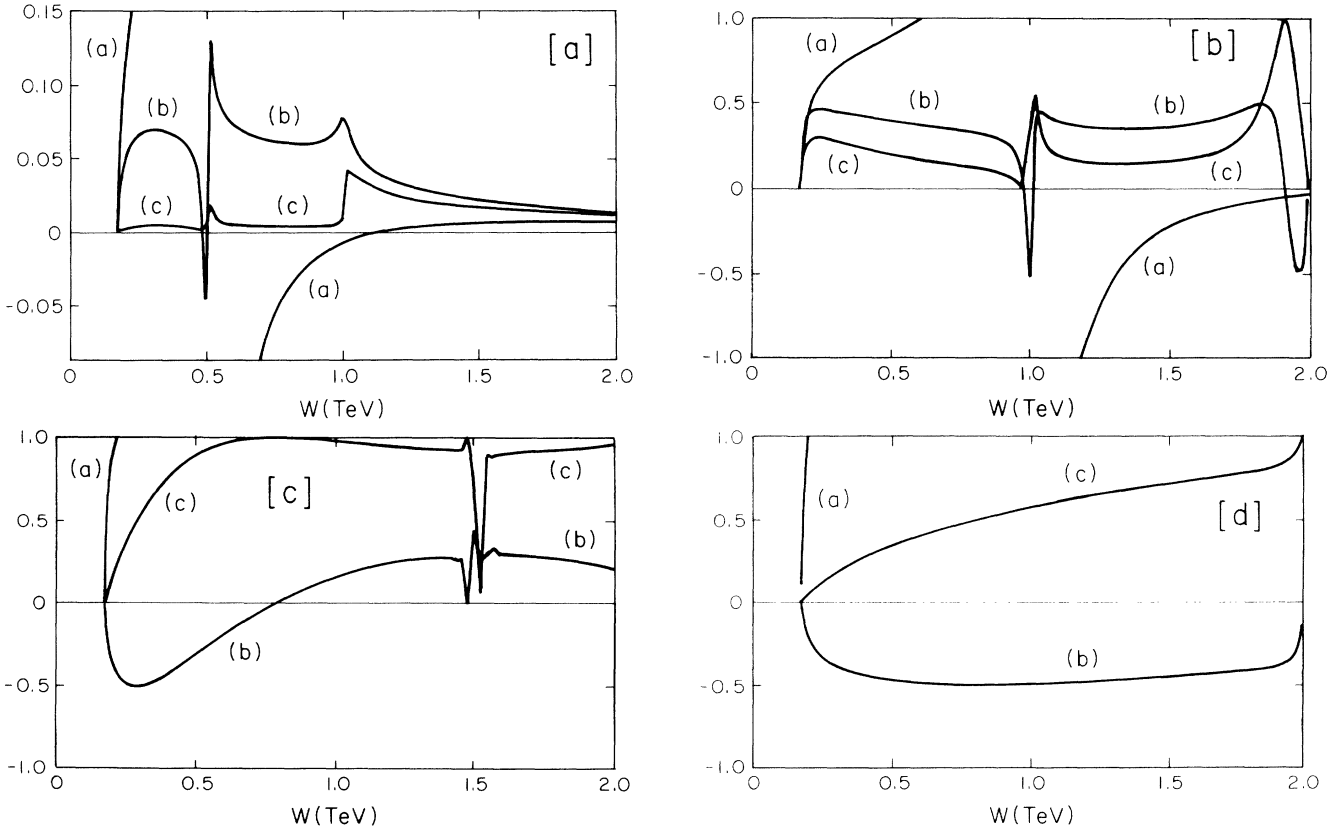

FIG. 3. The same as Fig. 2, except for the addition of a direct channel elementary particle ($\alpha_P = 1$).

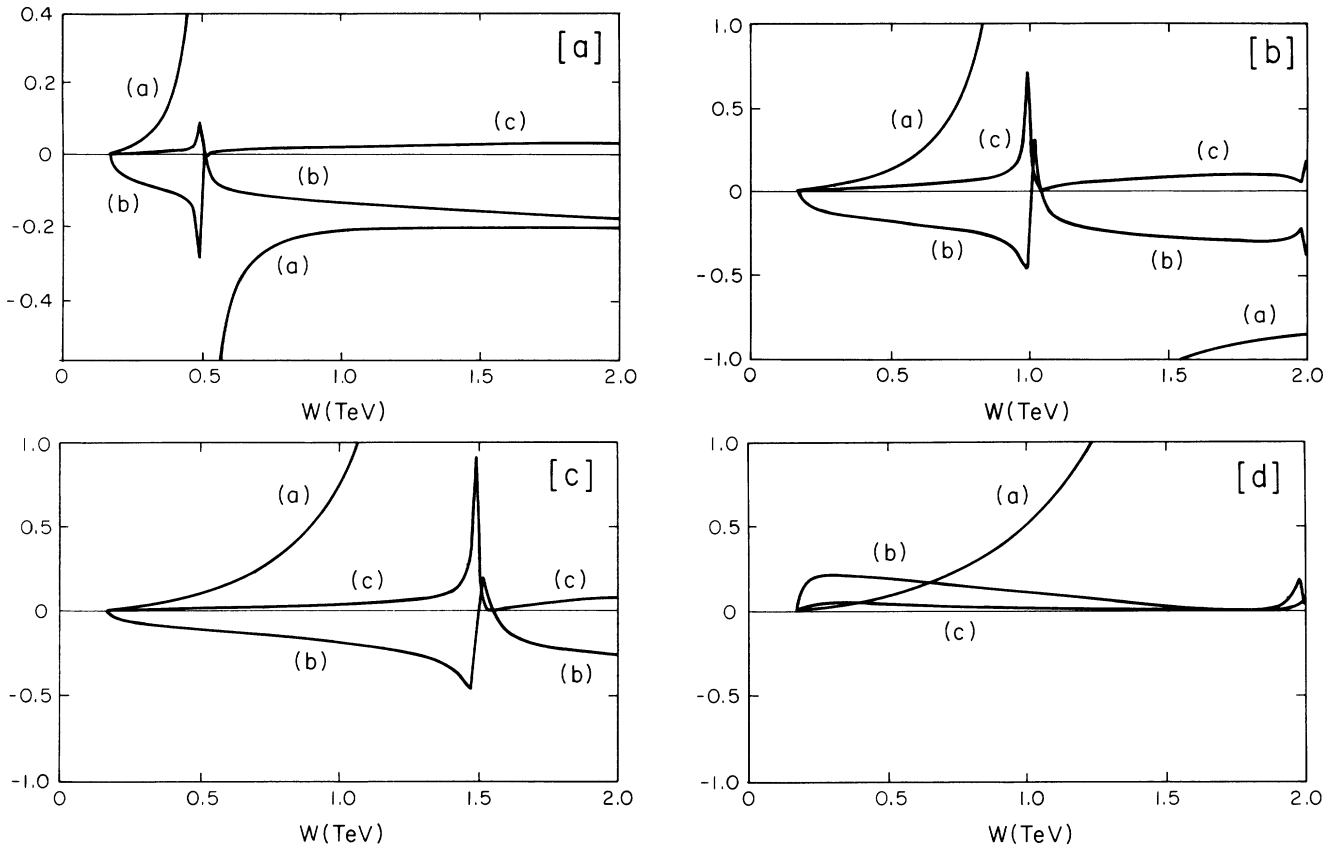

FIG. 4. The effect of unitarizing the full field theory potential. That is, the same as Fig. 3 except that $\alpha_4 = 1$.

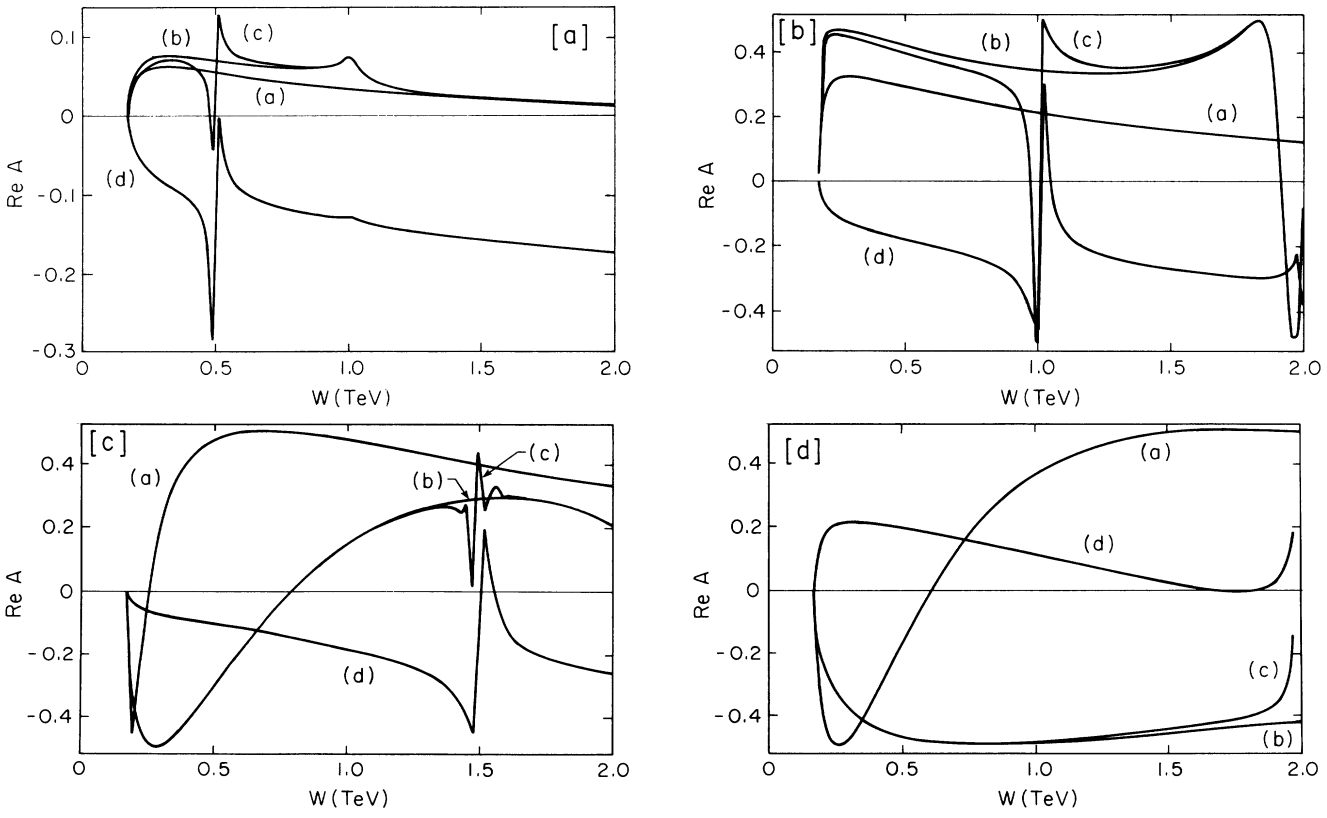

FIG. 5. The real part of the amplitude. The curves (a)–(d) correspond to the four cases (A)–(D) discussed in the text. (a)–(d) correspond to m_H equal 0.5, 1.0, 1.5, and 2.0 TeV.

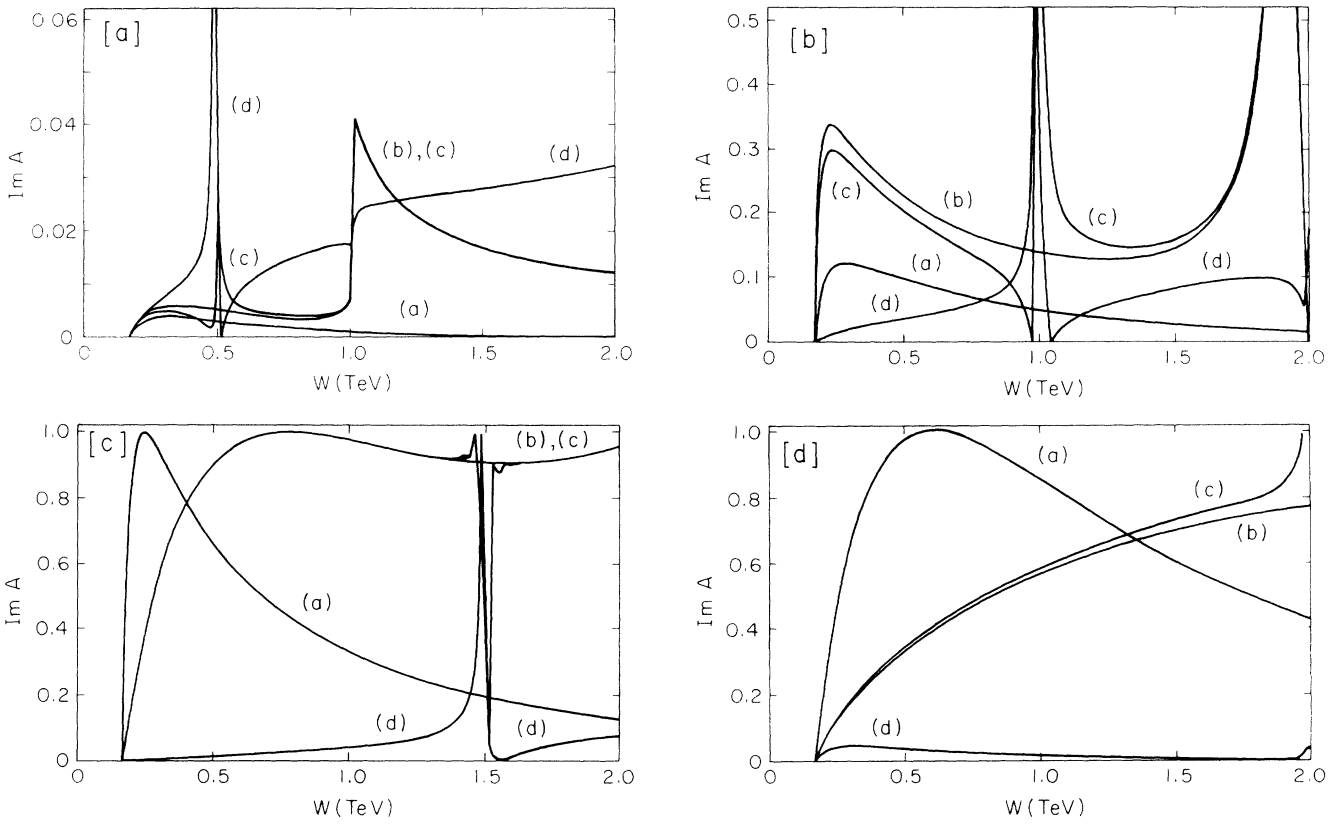

FIG. 6. The same as Fig. 5, except for the imaginary part of the amplitude.

$N_1=50$, 70, and 80. The results were as follows. The solutions are mostly insensitive to the relative distribution of points between the region $(2m_V, 2m_H)$ and $(2m_H, W_1)$. They tend to vary predictably with the strip width—a higher strip width corresponds to greater attraction and hence a deeper bound state and a larger energy value for the point at which the phase shift decreases through $\pi/2$. In case (A) there is essentially no change for any of the four mass values in the eight excursions. In the other cases sensitivities develop, particularly near $W=1$ TeV for $m_H=0.5$ TeV, and, more generally, $m_H=1.5$ and 2.0 TeV in the presence of the elementary particle pole. Figure 7 compares the results for a "typical" sensitive case. It shows the nine curves for $m_H=1.5$ TeV for case (C). The three "minority" curves have $W_1=3m_H$.

Finally we turn to the question of the residue of the bound-state pole in the $V_L V_L$ channel. If we find a Higgs-like particle below $2m_V$, will we be able to distinguish whether it is a $(V_L V_L)$ bound state or the elementary Higgs boson in the SM Lagrangian? Our calculations indicate that coupling constant magnitude might distinguish these two cases to the extent we can measure the residue at the pole in $V_L V_L$ scattering. From (2.6) the residue of the standard model Higgs boson is $\mathcal{R}\sim\frac{3}{2}\lambda_M m_H^2$. For a Higgs boson of 160 GeV, $\mathcal{R}$ is of the order of 3×10^{-4} TeV^2. For cases (A)–(C) the pole residue is of the order of 10^{-2} TeV^2 for this mass. For case (D) it is about 10^{-3} TeV^2. As the mass of the bound state decreases, the residue in our approximation increases, while the residue of an elementary Hills boson falls like m_H^2. This conclusion, however, could depend on details of the shape of the potential and hence probably should not be considered definitive. Table III gives a few values for the four potential choices. This result raises the possibility that the Higgs signal in the intermediate mass region ($<2m_V$) could be much larger than the SM prediction if the Higgs boson being detected is a bound state rather than the elementary SM Higgs boson.

B. $I=1$ scattering

It is known that $I=0$ exchange does not give $I=1, J=1$ resonances or bound states. Hence, for completeness, we added to the Higgs exchange of (2.9) a vector exchange term given by

$$\tilde{V}_{J=1}^{I=1}(s)=\lambda_M\frac{m_V^2}{vm_H^4}\{(6v+5m_V^2)Q_1(z_V)+2v[\tfrac{2}{3}Q_2(z_V)+\tfrac{1}{3}Q_0(z_V)]\}\ , \quad (3.1)$$

where $z_V=1+4v/m_V^2$, $v=(s-4m_V^2)/4$, and the Q_j are Legendre functions of the second kind. The relative size of vector exchange is much larger for $I=1$ than for $I=0$ because for $I=1$ the Q_0 in V exchange falls off much less rapidly as v goes to zero. This tends to compensate, for lower m_H, at $W<m_H$ for the $(m_V/m_H)^4$ suppression of vector exchange. Figure 8 gives our results for (the real

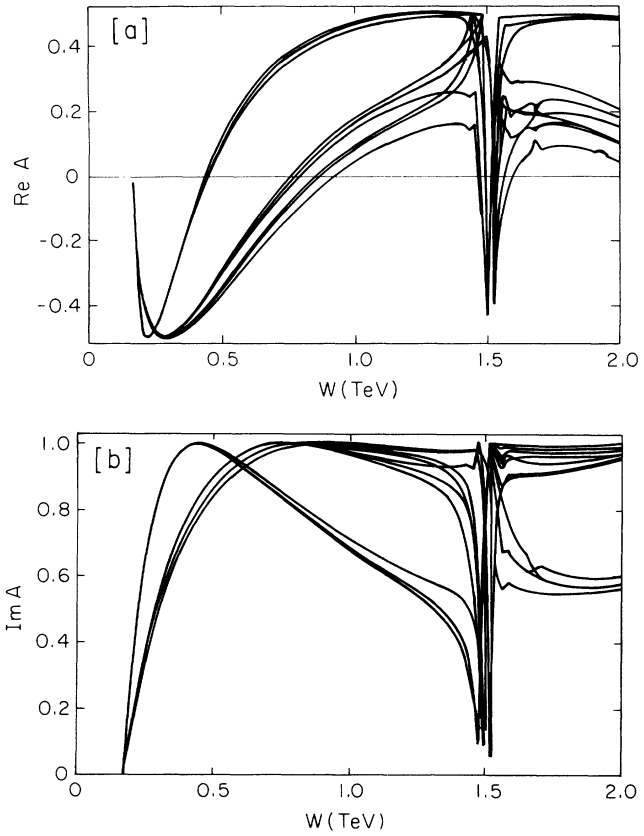

FIG. 7. The sensitivity of the results to the "strip width" W_1 [the upper limit of the integration in Eqs. (2.4) and (2.5)], and to the number of points used between $2m_V$ and $2m_H$ for a "sensitive" case. (a) shows the real part of the amplitude; (b) gives the imaginary part. The three "minority" curves have $W_1=3m_H$.

part of) $I=J=1$ scattering. The imaginary part is essentially zero and the potential is essentially equal to the real part of the amplitude.

C. $I=2$ scattering

As with $I=1$, $I=2$ scattering is a single channel calculation. As with $I=0$ there is a choice in the potential between (i) the analytic continuation of the potential from high J to $J=0$ or (ii) the field theory (SM) tree diagrams. If choice (i) is made the result is just that of choice (A) in Sec. III A above. That is, the contribution to $I=0$ and $I=2$ scattering of the t- and u-channel poles is identical so that the scattering is that of Figs. 1(a)–1(d) for the four different values of m_H (0.5, 1.0, 1.5, and 2.0 TeV). There is, of course, no $I=2$ elementary particle pole since in the SM there is no elementary $I=2$ Higgs boson. In the $I=2$ case bound-state poles occur below the V_LV_L threshold for $m_H>1.4$ TeV. This is just as with the case of $I=0$, case (A).

For case (ii) the situation is distinct from that of $I=0$. The potential is that of case (i) less a constant term as displayed in Eq. (2.10). The result for the real part of the scattering amplitude for the four m_H values cited is given in Fig. 9. The result for the m_H value at which bound states appear is very similar to that of case (D) with $I=0$. The $I=2$ field theory potential differs from the $I=0$ one in the absence of the elementary particle pole and its associated repulsive constant term:

$$\frac{-s}{s-m^2}=\frac{-m^2}{s-m^2}-1\ .$$

The result is that, as m_H increases, a bound state appears at threshold for $m_H=2.3$ TeV [about the same as $I=0$, case (D)]; it moves to negative s values for $m_H=2.6$ TeV.

IV. DISCUSSION

We have considered coupled channel V_LV_L and HH scattering in the N/D approximation along the lines of a number of dynamical calculations listed in Sec. I above. There are, of course, a variety of other approaches to the problem such as those recently reviewed by Chanowitz [19].

From the results of Sec. III, we see that, for an elementary Higgs boson of mass less than 1 TeV, N/D unitarization predicts very little nonresonant background in VV scattering below 2 TeV. This conclusion is clear from Figs. 6(a) and 6(b), augmented by Figs. 8 and 9. It is essentially independent of the choice made, among the potential cases investigated in Sec. III, for the potential in s-wave scattering.

For Higgs boson masses in the region above 1 TeV the results do depend on the assumptions about the potential. Assuming that the "correct" potential is the full field theory tree amplitude, our results are that, in spite of the large values of the potential in Figs. 4(c) and 4(d), the unitarized amplitudes for $m_H=1.5$ and $m_H=2$ TeV contain a narrowed Higgs bound state.

On the other hand, if the appropriate potential is that obtained from analytic continuation from high J to $J=0$ [with a simple pole added for the elementary Higgs case (C)] then the (narrowed) elementary Higgs boson is accompanied, as m_H approaches 1.2 TeV, by increasing strong scattering just above the VV threshold. For $m_H>1.2$ TeV a bound state develops at the VV threshold and for increasing m_H the bound state moves to smaller s, eventually becoming a tachyon. A VV bound state would be distinguishable from a low-mass elementary Higgs boson because its residue would be greater, with the ratio increasing as the binding deepens.

TABLE III. Residues at the bound state for cases (A)–(D).

Bound state mass (TeV)	Res(A)	Res(B)	Res(C)	Res(D)	Res(SM)
0.16	0.01	6×10^{-3}	7×10^{-3}	8×10^{-4}	3×10^{-4}
0.13	0.05	0.03	0.03	3×10^{-3}	1.3×10^{-4}
0.11	0.08	0.05	0.06	4×10^{-3}	8×10^{-5}

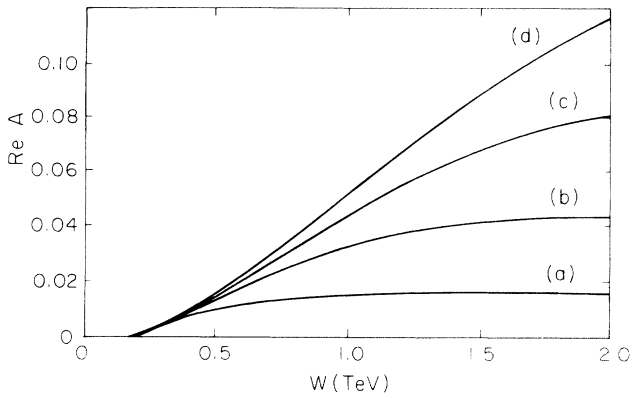

FIG. 8. The real part of the amplitude for $I=J=1$ scattering. The curves (a)–(d) assume m_H equal 0.5, 1.0, 1.5, and 2.0 TeV.

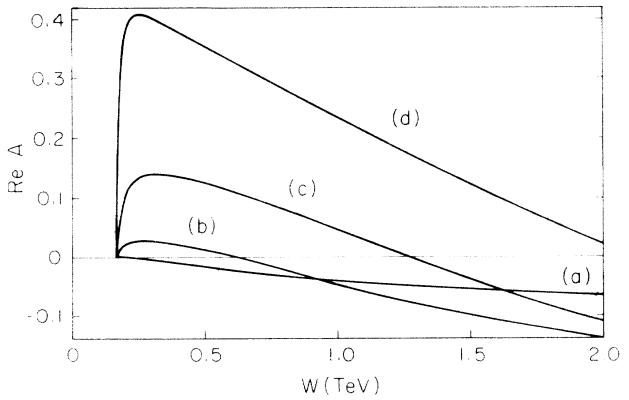

FIG. 9. The amplitude for $I=2$ scattering, with the potential of Lee, Quigg, and Thacker [2]. Again the curves (a)–(d) use m_H equal to 0.5, 1.0, 1.5, and 2.0 TeV. The real part is in (a), the imaginary part in (b).

A major feature of the results is the narrowing of the elementary Higgs width. As is clear from, for example, curves (c) and (d) of Figs. 6(a)–6(c), the unitary amplitudes generated by the N/D procedure give widths for the peaks in the $I=J=0$ amplitude far less than the values predicted on the basis of the potentials of (2.6). At $m_H=1.5$ TeV, Eq. (2.6) would predict a width well in excess of 1 TeV, an essentially unobservable resonance, while Fig. 6(c) shows a striking resonance peak of width well under 100 GeV. This narrowing could be an artifact of our approximations; however, it should be noted that such narrowing would violate no known principle such as analyticity or unitarity.

Our results may be compared with dynamical calculations that use the K-matrix or Padé approximants to unitarize [6,7,8]. For the K-matrix case the only output resonance is the input resonance and the input width is preserved. For the Padé case the output resonance is the input resonance for $m_H \lesssim 2.6$ TeV. For higher m_H the position of the output resonance falls below m_H, increasingly so with growing m_H. The output width is of the same order of magnitude but somewhat smaller than the width of an elementary Higgs boson at that output mass.

It is important to note that our use of the inelastic channel HH in VV scattering is only a first approximation to the effects of inelasticity. We have neglected the whole series of nV thresholds ($n=3,4,\ldots$). Each of these would be expected to add further attraction to $V_L V_L$ scattering similar in form to that of the HH channel but beginning at significantly lower energy. The result could well be "Reggeization" of $V_L V_L$ scattering, with a requirement to carry over to VV scattering much of the panoply of "classical" strong interaction scattering complications if a dynamical understanding of the VV scattering is to be achieved.

In summary, we have checked the original conjecture of Lee, Quigg, and Thacker [2] that, for large m_H, $V_L V_L$ scattering would manifest a low-mass s-wave bound state in the N/D method; we have shown that such a bound state does not occur until m_H reaches 2.3 TeV for the Lee potential choice. We have investigated $V_L V_L$ scattering for $I=0$, 1, and 2 including the effects of one inelastic channel (HH), for two plausible candidates for the potential, in addition to that of Lee, Quigg, and Thacker. For these other candidates a low-mass, $I=0$ bound state occurs at significantly lower values of m_H (1.2–1.4 TeV). In all cases, p-wave scattering is small. $I=2$ scattering is close to $I=0$ scattering because the two potentials are essentially identical except for the direct-channel elementary Higgs pole. The figures provide quantitative results for use in estimating event rates. Table III compares the width of a bound state Higgs boson with that of an elementary standard model Higgs boson. We note the dramatic narrowing of a TeV range Higgs boson that may be a consequence of the unitarity condition.

ACKNOWLEDGMENTS

It is a pleasure to acknowledge helpful conversations with K. Igi, F. Olness, F. Paige, C. Quigg, D. Rosenbaum, R. Vega, and S. Willenbrock, as well as computer assistance from B. Grinstein and F. Olness. We are particularly grateful to J. Uretsky who checked some of our results and in so doing made a major contribution by finding the factor of 2 difference between our amplitudes and those of Lee, Quigg, and Thacker. One of us (V.L.T.) benefited immensely from a large number of conversations on N/D methods with Professor Geoffrey Chew a generation ago and also from a recent conversation on this work.

[1] D. Dicus and V. Mathur, Phys. Rev. D 7, 3111 (1973).
[2] B. W. Lee, C. Quigg, and H. B. Thacker, Phys. Rev. D **16**, 1519 (1977).
[3] A. P. Contogouris, N. Mebarki, D. Atwood, and H. Tanaka, Mod. Phys. Lett. A **3**, 295 (1988) and A. P. Contogouris, N. Mebarki, and D. Atwood, in *From Colliders to Supercolliders,* Proceedings of the Workshop, Madison, Wisconsin, 1987, edited by V. Barger and F. Halzen

(World Scientific, Singapore, 1987).
[4] K. Hikasa and K. Igi, Phys. Lett. B **261**, 285 (1991).
[5] D. Sivers and J. L. Uretsky, Phys. Rev. Lett. **68**, 1649 (1992).
[6] W. W. Repko and C. J. Suchyta III, Phys. Rev. Lett. **62**, 859 (1989); D. A. Dicus and W. W. Repko, Phys. Lett. B **228**, 503 (1989).
[7] T. N. Truong, Phys. Rev. Lett. **61**, 2256 (1988); A. Dobado, M. J. Herrero, and T. N. Truong, Phys. Lett. B **235**, 129 (1990); **235**, 134 (1990). Also see S. Willenbrock, Phys. Rev. D **43**, 1710 (1990).
[8] D. A. Dicus and W. W. Repko, Phys. Rev. D **42**, 3660 (1990); **44**, 3473 (1991); **47**, 4154 (1993).
[9] H. Veltman and M. Veltman, Acta. Phys. Pol. **B22**, 669 (1991).
[10] C. B. Chiu, E. C. G. Sudarshan, and G. Bhamathi, Phys. Rev. D **45**, 844 (1992).
[11] L. A. P. Balázs, Phys. Rev. D **48**, 1310 (1993).
[12] D. Atkinson, M. Harada, and A. I. Sanda, Phys. Rev. D **46**, 3884 (1992).
[13] J.-L. Basdevant, E. Berger, D. Dicus, C. Kao, and S. Willenbrock, Phys. Lett. B **313**, 402 (1993).
[14] J. Uretsky, Phys. Rev. **123**, 1459 (1961); C. F. Chew, *The Analytic S-Matrix* (Benjamin, New York, 1966).
[15] See, for example, S. C. Frautschi, *Regge Poles and S-Matrix Theory* (Benjamin, New York, 1963).
[16] G. F. Chew and S. Mandelstam, Phys. Rev. **119**, 467 (1960).
[17] L. Castillejo, R. H. Dalitz, and F. J. Dyson, Phys. Rev. **101**, 453 (1956).
[18] N. Levinson, K. Dan. Vidensk. Selsk. Mat.-Fys. Medd. **25** (9) (1949).
[19] M. Chanowitz, in *Proceedings of the XXVI International Conference on High Energy Physics,* Dallas, Texas, 1992, edited by J. Sanford, AIP Conf. Proc. No. 272 (AIP, New York, 1993).